# Plasmid Releasing Multiple Channel Bridges for Transgene Expression After Spinal Cord Injury

Laura De Laporte[1], Yang Yang[1], Marina L Zelivyanskaya[1], Brian J Cummings[2,3], Aileen J Anderson[2,3] and Lonnie D Shea[1]

*[1]Department of Chemical and Biological Engineering, Northwestern University, Evanston, Illinois, USA; [2]Department of Physical Medicine and Rehabilitation, University of California, Irvine, California, USA; [3]Reeve-Irvine Research Center, Irvine, California, USA*

The regeneration of tissues with complex architectures requires strategies that promote the appropriate cellular processes, and can direct their organization. Plasmid-loaded multiple channel bridges were engineered for spinal cord regeneration with the ability to support and direct cellular processes and promote gene transfer at the injury site. The bridges were manufactured with a gas foaming technique, and had multiple channels with controllable diameter and encapsulated plasmid. Initial studies investigating bridge implantation subcutaneously (SC) indicated transgene expression *in vivo* for 44 days, with gene expression dependent upon the pore size of the bridge. In the rat spinal cord, bridges implanted into a lateral hemisection supported substantial cell infiltration, aligned cells within the channels, axon growth across the channels, and high levels of transgene expression at the implant site with decreasing levels rostral and caudal. Immunohistochemistry revealed that the transfected cells at the implant site were present in both the pores and channels of the bridge and were mainly identified as Schwann cells, fibroblasts, and macrophages, in descending order of transfection. This synergy between gene delivery and the scaffold architecture may enable the engineering of tissues with complex architectures.

*Received 14 February 2008; accepted 17 October 2008; published online 2 December 2008. doi:10.1038/mt.2008.252*

## INTRODUCTION

Regenerative medicine aims to control the local microenvironment as a means to support the development of functional tissues from endogenous or exogenous progenitor cells. Biomaterials serve a central role by providing a scaffold for cell infiltration or transplantation. Scaffolds designed with a complex architecture and the ability to function as a gene delivery vehicle may enhance tissue regeneration and repair by having the cellular processes induced by transgene expression synergize with the cellular organization directed by the structure. These scaffolds may be able to recreate complex tissue architectures, such as branching networks of the vascular or nervous systems, or an injury at the bone/cartilage interface. An example of this structure–function synergy involves the implantation of autologous peripheral nerve grafts at a spinal cord injury, which promotes and directs axonal elongation as a result of the graft architecture and factors secreted by cells within the graft.[1,2]

Bridges made from natural and synthetic biomaterials are being developed to promote regeneration after spinal cord injury, as the peripheral nerve grafts have limited clinical potential. The bridges are formed as gels or porous structures that can be either injected or implanted[3,4] to stabilize the injury site, prevent cavity formation that can occur secondary to the injury, limit scar formation, allow for cell infiltration and adhesion, or serve as a vehicle for drug delivery and cell transplantation.[5] More recently, bridges have been fabricated with multiple channels that are proposed to induce linear nerve growth through the bridge.[6–10]

Drug delivery from scaffolds can promote specific cellular processes, such as angiogenesis to enhance vascularization of the regenerating tissue. For spinal cord repair/regeneration, therapeutic factors include growth factors (*e.g.*, neurotrophins), factors targeting inhibitory molecules (*e.g.*, chondroitinase), and anti-inflammatory drugs.[11] The potential of drug delivery bridges for spinal cord regeneration/repair[9,10,12,13] was exemplified by a recent study that delivered chondroitinase to degrade chondroitin sulfates, along with a peripheral nerve graft, and resulted in axonal growth from above the injury site, through the graft, and back into the spinal cord.[14] However, designing effective drug delivery systems in the spinal cord that maintain therapeutic concentrations in conjunction with a physical support remains challenging, partly due to clearance by the cerebrospinal fluid. Bridges delivering gene therapy vectors may have the potential to overcome these challenges,[15] as polymer scaffolds loaded with nonviral vectors transfected endogenous cells subcutaneously (SC) resulting in transgene expression over 3 months.[16,17] Although gene delivery from biomaterials has been reported in the central nervous system within the optic nerve,[18] bridges capable of localized gene delivery have, to our knowledge, not been applied for spinal cord injury.

This study investigates the feasibility of plasmid delivery from bridges containing multiple longitudinal channels for nerve regeneration, and a porosity allowing for fluid transport and cell infiltration. Plasmid releasing bridges were fabricated using a gas foaming method and characterized for implantation in a spinal cord hemisection injury. They have an engineered structure

***Correspondence:*** *Lonnie D. Shea, Department of Chemical Engineering, Northwestern University, 2145 Sheridan Road/E156, Evanston, Illinois 60208-3120, USA. E-mail: l-shea@northwestern.edu*

to promote and direct cell organization and regeneration, and locally deliver plasmid to induce transgene expression in the spinal cord. Reporter genes were used to characterize the levels and duration of transgene expression and the location and identity of transfected cells after implantation of the bridge in the spinal cord. Future studies will test the delivery of plasmids encoding for functional proteins, such as neurotrophic factors or chondroitinase. Ultimately, the synergy between a scaffold architecture and gene delivery, providing a combination of physical and chemical guidance cues, has the potential to stimulate spinal cord repair and enable the regeneration of a variety of tissues with complex architectures.

## RESULTS

### Design and characterization of DNA-loaded multiple channel bridges

Porous multiple channel bridges with a defined asymmetrical structure were developed, and designed to serve as a vehicle for localized gene delivery. The biodegradable polymer, poly(lactide-co-glycolide) (PLG), was used for bridge fabrication using a gas foaming method[16,19] that was adapted to enable the formation of complex structures with channels of controllable diameter. A mold was designed to create bridges with either 7 or 20 channels of 250 or 150 μm diameter, respectively, with the number of channels limited by the spacing in the pin guides (**Figure 1a–c**). The dimensions of the bridge were 4 mm in length, 2.6 mm in width, and 1.5 mm in height, which matched the dimensions of the lateral hemisection created in the rat spinal cord[20] (**Figure 1d**). The bridges were >90% porous, with the porosity resulting from the channels created by the pins and the pores in the polymer, surrounding the channels, created by leaching the porogen (NaCl). The NaCl was sieved in different size ranges (<38, 38–63, 63–106, 106–250, and 250–425 μm), resulting in specific pore sizes. The maximum porogen size to fabricate bridges with 250- and 150-μm channels, respectively, was 106 and 63 μm, as larger sized porogen restricted solids packing between the pins.

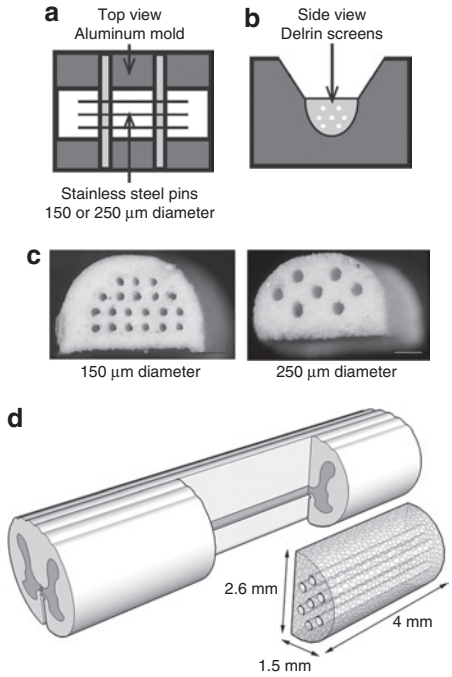


**Figure 1 Multiple channel bridges for spinal cord regeneration.** (**a**,**b**) Schematic of the aluminum mold, Delrin screens, and stainless steel pins to fabricate the multiple channel bridges: (**a**) top view and (**b**) side view. (**c**) Multiple channel bridges with 20 channels of 150 μm diameter and 7 channels of 250 μm diameter, scale bars = 500 μm. (**d**) Schematic of bridge implantation in spinal cord hemisection model.

### *In vitro* DNA release study

Subsequent studies investigated the plasmid encapsulation efficiency into the bridge, and the integrity and *in vitro* release of the encapsulated plasmid at 37 °C in phosphate-buffered saline. The plasmid release kinetics and integrity described here were obtained with bridges containing 250-μm diameter channels and pores in the 63–106 μm range. Plasmid incorporation, release, and integrity did not significantly vary with the pore size or channel diameter of the bridge. The efficiency of plasmid incorporation was 66.4 ± 3.2% of the initial amount used, with loss occurring primarily during the porogen leaching step. Approximately 75% of the DNA present in the bridge after leaching was released from the bridges after 1 day, with most of the remaining DNA being slowly released over the next 6 days. Less than 10% of the DNA remained in the bridge after 1 week (**Figure 2a**). The released plasmid was structurally intact, though a shift from the supercoiled to open conformation was observed (**Figure 2b**). The original plasmid was primarily supercoiled (89%), whereas the DNA released from the bridge after 1 day and 1 week contained DNA mostly in the open conformation (57 ± 1 and 61 ± 1%, respectively), with

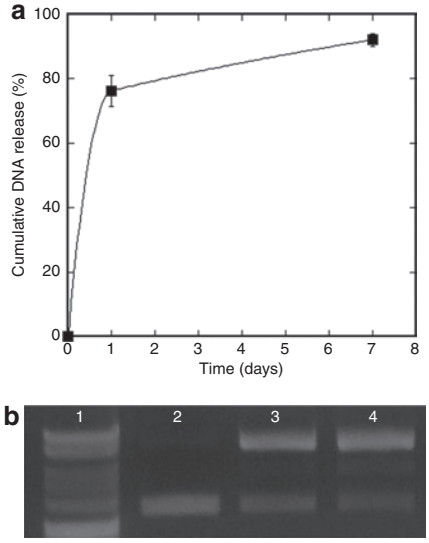


**Figure 2** ***In vitro*** **DNA release study from bridges with a pore size of 63–106 μm and 250-μm diameter channels (*n* = 6).** (**a**) Cumulative release, error bars represent SEs. (**b**) Agarose electrophoresis gel: line 1: 1-kb ladder, line 2: DNA before encapsulation into bridge, line 3: DNA released from bridge at 1 day (*n* = 3), and line 4: DNA released from bridge at 1 week (*n* = 3).

smaller amounts of supercoiled (32 ± 1, 25 ± 1%) and linear DNA (11 ± 0, 14 ± 1%). Both supercoiled and open conformations have been previously shown to produce high levels of transgene expression.[16]

## Transgene expression SC

Bridges containing 250-µm diameter channels were loaded with 800 µg of plasmids encoding for firefly luciferase and implanted SC in mice to allow for long-term monitoring of transgene expression using a Xenogen imaging system. DNA-loaded bridges with larger pore sizes resulted in more consistent and sustained transgene expression following implantation, and retained their integrity through the 44 days *in vivo*. For a pore size in the range of 63–106 µm ($n$ = 5), all mice implanted with the bridges expressed the luciferase protein for >44 days (**Figure 3**). The mice demonstrated consistent levels of transgene expression, with stable levels sustained from days 4 though 37, but decreasing 2.5-fold between days 37 and 44. In contrast, for a pore size in the range of 38–63 µm ($n$ = 5), only one of five mice implanted with a bridge had consistent transgene expression after 1 week. Accordingly, the average level of transgene expression for a pore size in the 63–106 µm range at 9 days was on the order of $10^6$ photons/s, while the average level of transgene expression for a pore size in the range of 38–63 µm at 9 days was on the order of $10^5$ photons/s, which is approximately fourfold over background. The group with smaller pore sizes did not consistently emit light at levels above background. These results revealed that DNA-loaded bridges locally induced high levels of transgene expression *in vivo* for a sustained period of time with a dependence of transgene expression on the pore size of the bridge. Based on our observations that larger pores consistently resulted in long-term SC transgene expression *in vivo*, and that 250-µm channels were required to fabricate stable bridges with larger pores, subsequent studies in a rat spinal cord hemisection model were performed with bridges containing 250-µm channels and a 63–106-µm pore size.

## Bridge implantation in rat spinal cord lateral hemisection injury model

The DNA-loaded bridges in this report were subsequently investigated for their ability to integrate into the spinal cord after injury, and locally deliver plasmid resulting in transgene expression at the injury site. Bridges were implanted in a rat spinal cord lateral hemisection model with the channels oriented parallel to the midline of the spinal cord (**Figure 1d**). Implanted bridges supported cell infiltration, resulting in tissue apposition after implantation 2 weeks postsurgery (**Figure 4a**). The bridge porosity resulted from the channels and the surrounding pores in the polymer, and when comparing the cells present in the pores (**Figure 4b**), the cells within the channels were oriented along the major axis of the channel (**Figure 4c**). Effective integration of the bridge within the spinal cord was further demonstrated by the ability of channels to support and direct axonal elongation (**Figure 4d**). At 12 weeks of implantation, axons were observed to span the implant site within the channels (**Figure 4e**). These data demonstrate that the bridge structure is able to stabilize the injury area and provide a favorable environment for spinal cord regeneration.

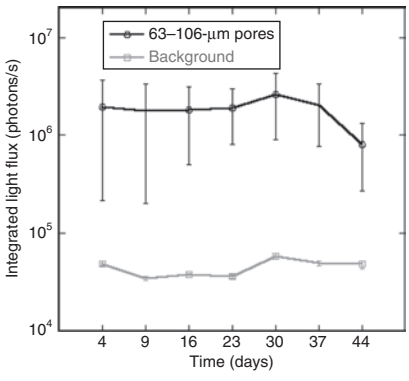


**Figure 3 Transgene expression in a mice subcutaneous model after implantation of bridges loaded with plasmid encoding for firefly luciferase.** Bridges reported on graph contained a pore size of 63–106 µm ($n$ = 5). Error bars represent SEs. An ANOVA with *post hoc* Wilcoxon one-way test demonstrated a significant difference between the experimental condition and background levels ($P < 0.02$).

## Transgene expression following bridge implantation

Transgene expression was observed in the spinal cord after implanting the plasmid loaded bridges in a hemisection injury model. Analysis of the luciferase expression in the spinal cord over time required retrieving implants at several time points, with the spinal cord tissue lysed and the luciferase protein measured using a luminometer. High levels of transgene expression were observed at the injury site 3 days after implantation, with levels dropping ~60% in the two spinal segments immediately rostral and caudal of the injury site (**Figure 5**), and the segments further away from the injury site only containing a few percent or less of the luciferase produced at the injury site.

Transgene expression decreased 10% between 3 days and 1 week, but reduced a hundred-fold between 1 and 2 weeks, with no detectable levels in the adjacent segments of the injury site at 2 weeks. Interestingly, a group of two rats demonstrated levels of transgene expression at day 1 that was sixfold higher relative to the levels observed at 3 days, but were not included in the graph because of the low sample number. These studies indicate that

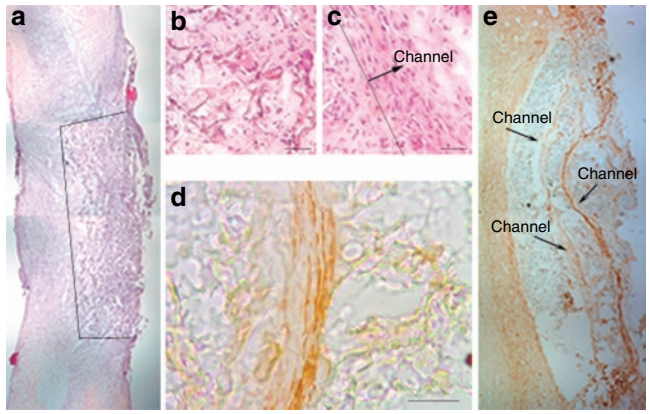


**Figure 4 Bridge implantation into a rat spinal cord lateral hemisection injury model.** (**a–c**) Hematoxylin eosin staining of bridges retrieved at 2 weeks of implantation: (**a**) Low-magnification image of a bridge implanted in the spinal cord hemisection model. The line marks the border between the bridge and tissue. (**b**) High-magnification image of cells within the bridge pore structure created by porogen, compared with the alignment of cells in channel of bridge (**c**). The line defines the edge of a channel with the arrow pointing in the direction of the channel, scale bar = 50 µm. (**d,e**) Neurofilament stain (NF200) for neurite growth at 12 weeks: (**d**) inside the channel, scale bar = 100 µm; (**e**) across the channels of the polymer bridge.

plasmid releasing bridges transfect cells in the spinal cord resulting in localized and sustained transgene expression.

## Distribution of transfected cells following bridge implantation

Subsequent experiments investigated the distribution of transfected cells within the bridge and surrounding tissue. Plasmid encoding for luciferase was replaced with plasmid encoding for enhanced green fluorescent protein (EGFP) to enable the visualization of transfected cells. The border of the polymer particles of the bridge was defined based on the appearance of the bridge under phase (**Figure 6a**). Endogenous cells infiltrating the porous bridge or present in the adjacent spinal cord tissue were transfected. After 1 week, transfected cells were observed aligned within the channels of the bridge (**Figure 6b**), adjacent to or on the polymer (P), and within the pores of the bridge (**Figure 6c–e**). Transfected cells were identified as both Hoechst (blue) and EGFP (green) positive (**Figure 6d,e**). A similar number of transfected cells were visualized in the tissue alongside the bridge, and located in the white (**Figure 6f**) and gray (**Figure 6g**) matter. After 2 weeks, EGFP positive cells were observed in similar regions, but in lesser amounts compared with the 1-week time point (**Figure 6h**). No EGFP positive cells were detected in histological sections of bridges implanted without encapsulated plasmid (**Figure 6i**).

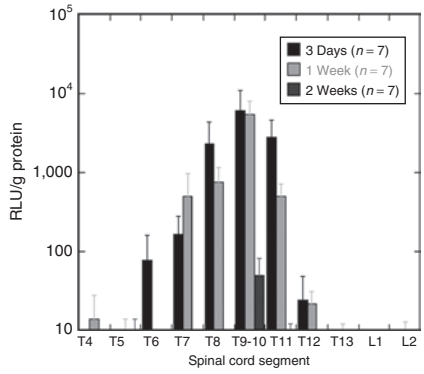


**Figure 5 Transgene expression in the rat spinal cord lateral hemisection model at three time points (3 days, 1 week, and 2 weeks) (*n* = 7).** Error bars represent SEs. RLU, relative light unit.

## Identification of cell types transfected within the bridge

The cell types that infiltrated the bridge after spinal cord injury were subsequently identified in order to determine the cell types transfected. Tissue sections were analyzed with a panel of antibodies to

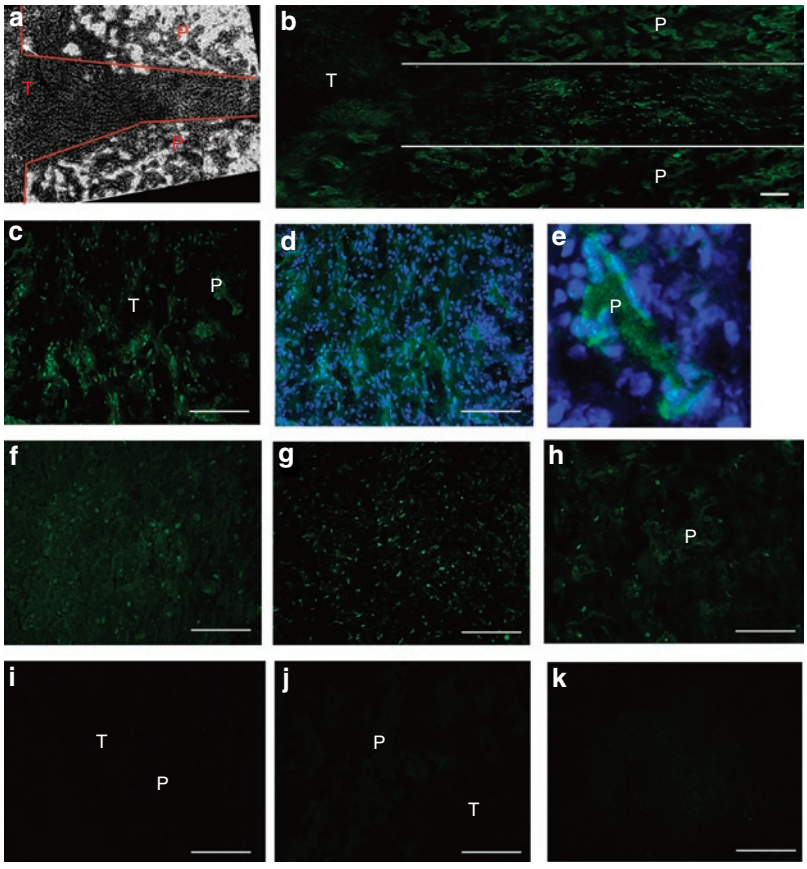


**Figure 6 Location of transfected cells after implantation of bridges loaded with plasmid encoding for enhanced green fluorescent protein (green).** The boundaries of the bridge were defined under phase (**a**). Transfected cells were observed aligned within the channels of the bridge (**b**), adjacent or on the polymer, and within the pores of the bridge (**c**). (**d,e**) Bridge after 1 week in the presence of a Hoechst stain (blue). (**f**) White and (**g**) gray matter of spinal cord tissue next to the implant site. Bridge after 2 weeks (**h**). Negative controls: implanted bridge that did not contain DNA (**i**), and stain of both the bridge (**j**) and its surrounding tissue (**k**) after eliminating the primary antibody. P, polymer; T, tissue. Scale bars = 100 µm.

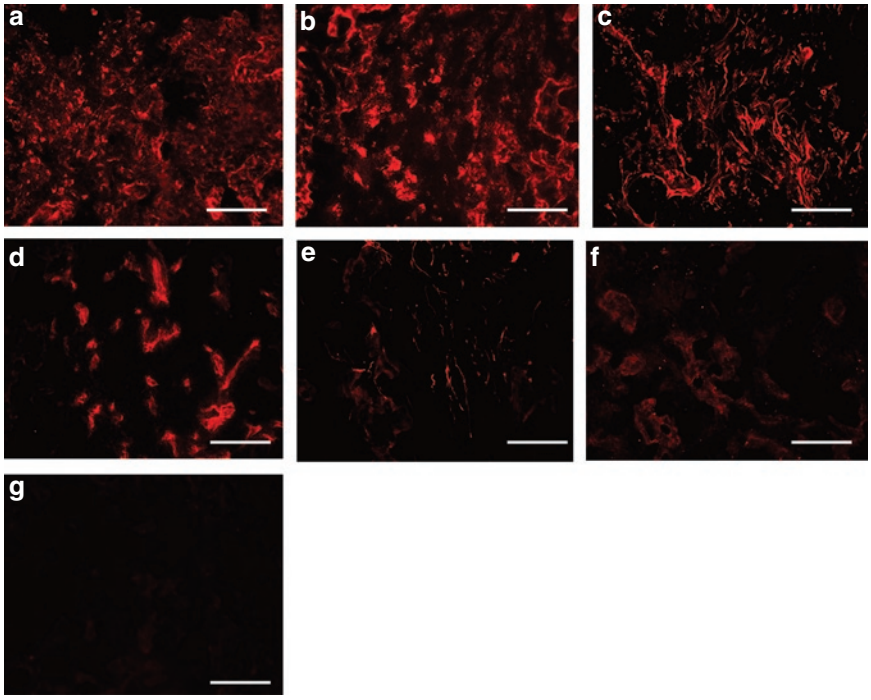


**Figure 7 Identification of cells infiltrating the bridge at 1 week.** Images captured for immunohistochemistry staining with antibodies to fibroblasts (rPH) (**a**), macrophages (ED-1) (**b**), Schwann cells (S100β) (**c**), endothelial cells (RECA) (**d**), astrocytes (GFAP) (**e**), or oligodendrocytes (RIP) (**f**). Negative controls: stain of bridge after eliminating the primary antibodies (**g**). Scale bars = 100 µm.

cell types commonly reported at a spinal cord injury [*i.e.*, Schwann cells, oligodendrocytes, macrophages, reactive astrocytes, fibroblasts, and endothelial cells (see Materials and Methods)]. The main cell types that infiltrated the bridge pores and channels were identified as fibroblasts, macrophages, and Schwann cells (**Figure 7a–c**), with endothelial cells being observed in the bridge construct in significantly lower quantities (**Figure 7d**). Reactive astrocytes, which usually dominate the scar tissue formed after spinal cord injury, mostly remained outside the bridge borders, though, a sparse number of reactive astrocytes were observed in the entrance of the channels (**Figure 7e**). Few oligodendrocytes (*i.e.*, myelinating glial cell type in central nervous system) were detected in the bridge (**Figure 7f**).

Because fibroblasts, macrophages, Schwann cells, and endothelial cells were most prevalent in the bridge, tissue sections were double stained with antibodies to EGFP and the cell-specific antigens to determine the identity of the transfected cells (**Figure 8a–d**). Fibroblast, Schwann cell, and macrophage immunostaining revealed a large number of cells that were stained positively for both EGFP and these respective antibodies; these were further analyzed and quantified by calculating the percentages of the number of transfected cells that were identified as that specific cell type (**Figure 8e**). The percentages of transfected cell identified as Schwann cells, fibroblasts, and macrophages were ~41 ± 4, 30 ± 5, and 24 ± 6%, respectively, with Schwann cells being transfected in significantly greater numbers than fibroblasts and macrophages.

## DISCUSSION

The field of tissue engineering requires scaffolds that are able to regenerate tissues with complex architectures. For neural tissue engineering applications, scaffolds should be designed to orient regenerating nerves,[11] and the presence of multiple linear channels has been proposed to guide and orient axonal elongation.[7,9,21] In this report, DNA-loaded multiple channel bridges were developed with the goal of investigating a permissive environment for spinal cord regeneration by providing a combination of physical and chemical guidance cues for extending neurites. The bridges were made of PLG, which is biodegradable and has demonstrated biocompatibility with the spinal cord.[22] Porous PLG scaffolds have previously been implanted in the spinal cord resulting in a reduction of scar formation and improved functional recovery.[20] The physical channel configuration of the bridges used in this report supported axon growth across the 4-mm long injury site, which suggests longitudinal guidance of regenerating axons.[4]

The combination of multiple channel bridges with gene therapy has the potential to provide architectural control and deliver plasmid to the host cells, which then function as bioreactors to locally provide long-term protein expression at effective concentrations. Relative to protein releasing systems, localized plasmid release in the spinal cord could provide a versatile tool to induce the prolonged expression of one or more therapeutic factors lacking at the injury site. Therapeutic factors that have been delivered after spinal cord injury include neurotrophic factors (*e.g.*, neurotrophin-3,[13,23,24] brain-derived neurotrophic factor,[25] basic fibroblast growth factor[26]) that stimulate neuron survival and axon outgrowth, or reduce secondary injury,[27] antibodies (*e.g.*, nogo-neutralizing antibody IN-1[28]) or enzymes (*e.g.*, chondroitinase[14]) that block or degrade inhibitory factors, mitogens or differentiation factors that manipulate the presence

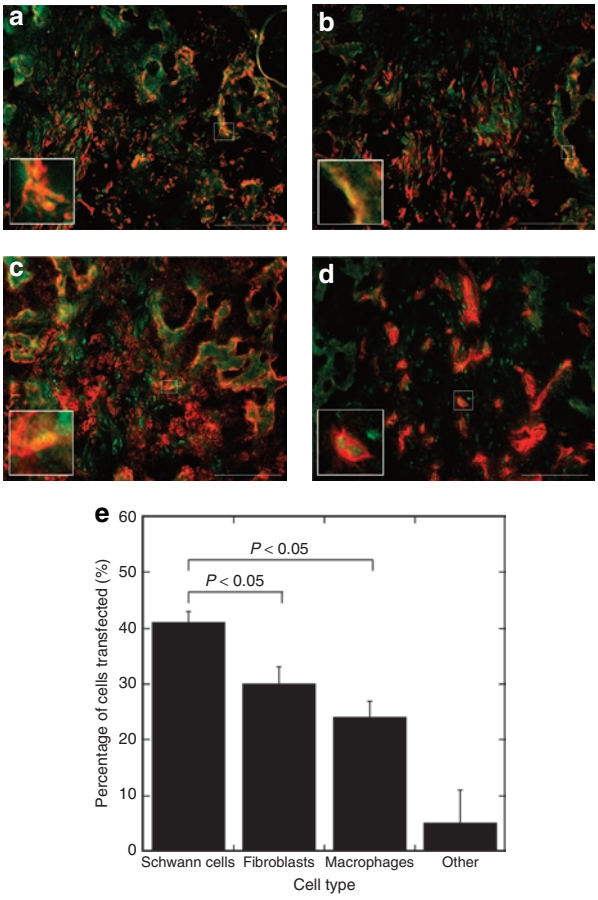


**Figure 8 Identification of transfected cells in the bridge.** Double staining of slides with antibodies to EGFP (green) and to a specific cell type (red). Images were taken for antibody staining with S100β (**a**), rPH (**b**), ED-1 (**c**), or RECA (**d**). Scale bars = 100 µm. The cells marked by the white squares were magnified in the left corner of each picture. (**e**) Percentages of transfected cells identified as a specific cell type. An ANOVA with Tukey *post hoc* test was performed demonstrating that the percentage of transfected cells identified as Schwann cells was statistically higher than for fibroblasts and macrophages ($P < 0.05$). Error bars represent SEs.

of regenerative cells types (*e.g.*, astrocytes, oligodendrocytes),[29–31] and anti-inflammatory drugs.[11]

The delivery of drugs to the spinal cord is mostly performed by a catheter associated with osmotic pumps used for intrathecal drug administration.[24,32] However, this method requires additional surgery to remove the catheter, and it is challenging to control the location, amount, and residence time of the drugs. The catheters can clog, may damage the spinal cord, and likely provide the highest concentration at a site adjacent to the injury. Sustained drug delivery from biomaterial bridges may overcome some of these challenges and obtain a local and sustained presence of bioactive factors during their therapeutic timeframe without having to rely on invasive removal methods that could evoke inflammatory responses. Localized delivery from bridges may reduce the quantity of drug required to maintain the desired drug concentrations at the target site.[33] Protein releasing hydrogels have been injected or implanted at a spinal cord injury,[12,13,26] but may have difficulties maintaining a desired concentration profile. Relative to traditional drug delivery systems, genetics-based approaches have the potential to provide and maintain the local concentration of diffusible factors.[15] DNA has been delivered to the spinal cord with a direct injection of viral and nonviral vectors or ultrasound,[34–38] but has not elicited the pattern of transfection demonstrated here, and has not been performed within the context of a structure to guide regeneration. As an alternative gene therapy approach for spinal cord regeneration, cells that have been genetically engineered to secrete a variety of neurotrophic factors have been transplanted.[39–41] However, delivery efficiency, cell migration and survival, and the inflammatory response are complicating factors that have limited success thus far.

The DNA-loaded bridges produced prolonged expression *in vivo* for both SC and spinal cord implants, with significantly different expression profiles. Expression was dependent on the pore size of the bridge, which may occur due to alterations in the rate of cell infiltration,[42] as release studies did not indicate a pore size dependence. Additionally, the expression profile can be influenced by the cell types transfected. In the spinal cord, the duration of expression persisted for 2 weeks, with the cells transfected by the released plasmid being primarily identified as S100β, rPH, and ED-1 positive, listed in descending order of transfection. Macrophages and fibroblasts are hypothesized to be transfected by nonviral gene delivery from a biomaterial,[17] as they are characteristic of the foreign body response that occurs following implantation of a material. Macrophages typically arrive within the first days, and are present for a time scale of days to weeks.[43] Fibroblasts, Schwann cells, and endothelial cells typically arrive after macrophages from outside the central nervous system and can reside at the implant site for several weeks. An additional factor limiting the duration of transgene expression is likely the CpG dinucleotides that mediate an inflammatory response.[44]

Transgene expression was highest at the implant site, yet transfection was also observed in the segments adjacent to the implant. For SC implantation, bioluminescence imaging and immunohistochemical staining indicated localized expression within 100 µm of the implant site.[16,17,19,45] However, in the spinal cord, expression was observed in adjacent segments that are centimeters away from the implant site. Transfection in the adjacent segments may be beneficial as expression in these segments could be employed to promote neuron survival outside the injury site. Additionally, this expression pattern could create a concentration gradient, with the highest concentration within the bridge, which could direct axon elongation toward the injury, into and across the bridge.[46,47] The constant exchange of cerebrospinal fluid in the spinal cord may transport plasmid into the adjacent segments, which may also be a factor that reduces the duration of expression relative to SC implantation.

Gene delivery is a versatile approach that could be employed to target a range of cellular responses associated with spinal cord injury response or regeneration. The days following injury is a critical period during which substantial cell death can occur, and expression of therapeutic factors may mitigate this response to allow a more robust regeneration. Currently, the standard therapy for treating spinal cord injury is the injection of methylprednisolone to minimize inflammation and reduce secondary injury,[48] and gene delivery could similarly target inflammation. Alternatively,

delivery of genes encoding for growth and differentiation factors may limit neuron death and initiate axonal outgrowth, or could be employed along with cell transplantation.[29–31,49] The level and duration of transgene expression necessary for therapeutic efficacy will vary depending on the protein. Though the specific targets for therapy remain unknown because of the complexity of the host response, transient expression is likely desirable. Expression of regenerative factors at the implant site can induce axonal growth in the bridge, yet should subside to encourage axonal re-entry into the host tissue.[3]

The regeneration of complex tissues such as spinal cord is expected to require multiple signals that can promote and organize tissue formation. In the spinal cord, peripheral nerve grafts supplemented with drug delivery have demonstrated the potential for synergy between structure and function.[14] However, the clinical potential of peripheral nerve grafts has been largely stalled, and motivates the development of synthetic bridges that deliver factors limiting cell death and promoting a regenerative response that can synergize with a structure to orient and guide axonal elongation. Synthetic systems have not demonstrated functional recovery to date, likely due to the inability to present the combination of factors that can block the inhibitory factors within the environment and provide the stimulatory factors to promote regeneration. The bridges in this report, capable of gene delivery within the spinal cord, can also be modified with extracellular matrix proteins and serve as vehicles for cell transplantation, for which the combination may provide the range of signals necessary to promote regeneration. Ongoing studies using these bridges with functional genes (*e.g.*, neurotrophic factors) are investigating the identity of regenerating axons and the ability to promote functional recovery. The synergy between gene delivery and the scaffold architecture may have broad applications in regenerative medicine involving complex architectures.

## MATERIALS AND METHODS

***Fabrication of DNA-loaded multiple channel bridges.*** DNA-loaded multiple channel bridges are fabricated with a gas foaming/particulate leaching method[50] using three main building blocks: plasmid, PLG microspheres, and porogen (NaCl). Plasmids encoding for either firefly luciferase or EGFP were produced with an Endofree Gigaprep (Qiagen, Valencia, CA) and 800 µg of DNA was lyophilized with 1 mg lactose as a cryoprotectant per bridge. PLG (75:25 mole ratio of D, L-lactide to glycolide: 50% by mass of 0.76 dl/g; Lakeshore Biomaterials, Birmingham, AL; 50% by mass of 0.20 dl/g; Boehringer Ingelheim, Ridgefield, CT) microspheres were made using a primary oil in water emulsion technique. Porogen of defined size was obtained by sieving NaCl particles (<38, 38–63, 63–106, 106–250, 250–425 µm; WS Tyler, Mentor, OH).

The solid mixture, with a porogen to polymer ratio of 4, was added layer by layer into a custom-made mold consisting of an aluminum base, two Delrin pin guides with predrilled holes, and stainless steel pins (150 or 250 µm diameter) using a wet granulation method (**Figure 1**). The mixture was compression molded (15 seconds at 200 psi) using a Carver Laboratory Press and placed into a custom-made pressure vessel, which was equilibrated with high pressure $CO_2$ (800 psi, 16 hours). The microspheres fused with a controlled $CO_2$ release rate of ~20 psi/min using a flow meter (Gilmont Instruments, Barrington, IL). The high pressure $CO_2$ has a sterilizing effect on the polymer,[17] and the multiple channel bridges were immersed in sterile water for 1 hour to leach the NaCl. The porosity was calculated as the ratio of the empty volume of the bridge over the total volume of the bridge based on its dimensions. The empty volume was calculated as the total volume minus the volume of the polymer, which was defined by the weight of the bridge over the PLG density (2.3 g/cm$^3$).

**In vitro *DNA release study*.** Multiple channel bridges ($n$ = 6) were fabricated with 50 µg of plasmid and the amount of DNA lost during the leaching step was measured with a fluorometer (Turner BioSystems, Sunnyvale, CA) and a Hoechst dye assay, which was then used to calculate the DNA incorporation efficiency. The release study was performed in 1 ml of phosphate-buffered saline stored at 37 °C. At multiple time points, the DNA released from the bridges was measured using the fluorometer. At the end of the release study, the bridges were dissolved in chloroform and the DNA was extracted to quantify the amount of DNA remaining in the bridge. The cumulative amount of DNA released at a time point is defined as the amount released through that time, normalized by the total amount of DNA released and extracted. The quality of the DNA released from the bridge was analyzed using agarose gel electrophoresis.

***SC mouse model.*** Bridges loaded with plasmid encoding for firefly luciferase were initially tested SC using 10 male CD1 mice (20–22 g; Charles River), which were treated according to the Animal Care and Use Committee guidelines at Northwestern University. Transgene expression was monitored in real-time using an IVIS Imaging System (Xenogen, Alameda, CA), which reduces the number of animals required.[16] Luciferin (150 mg/kg; Molecular Therapeutics, Ann Arbor, MI) was injected intraperitoneally at different time points resulting in the production of oxyluciferin and light, which is proportional to the amount of luciferase. The signal intensity was reported as an integrated light flux (photons/s).

***Rat spinal cord hemisection model.*** Thirty three female Long-Evans rats (180–200 g; Charles River) were treated according to the Animal Care and Use Committee guidelines at the University of California Irvine and Northwestern University. The rats were prehandled for 2 weeks before surgery. They were anesthetized using a combination of ketamine and xylazine (100 mg/kg ketamine, 10 mg/kg xylazine, intraperitoneal). A laminectomy was performed at T9-10 and a 4-mm long spinal cord segment, lateral of the midline, was removed to create a hemisection. The bridges were implanted in the injury space (**Figure 1d**) and covered by Gelfoam. The muscles were sutured together and the skin was stapled. Postoperative care consisted of the administration of Baytril (enrofloxacin 2.5 mg/kg SC, once a day for 2 weeks), buprenorphine (0.01 mg/kg SC, twice a day for 2 days), and lactate ringer solution (5 ml/100 g, once a day for 5 days). Bladders were expressed twice a day until bladder function recovery.

***Quantification of transgene expression in hemisection model.*** Bridges loaded with plasmid encoding for firefly luciferin were implanted into the spinal cord to quantify luciferase levels within defined segments. After 3 days, 1 week, and 2 weeks, rats ($n$ = 7) were euthanized and the fresh spinal segments (T4-L2) were retrieved and frozen. The spinal cord segments were thawed and cut into small pieces, 100 µl of lysis buffer (Cell Culture Lysis Reagent 1×; Promega, Madison, WI) was added, and the tissue was vortexed for 15 seconds and rotated for 30 minutes using a Rotamix (Appropriate Technical Resources, Laurel, MD). One freeze–thaw cycle was performed and the tissue lysate was centrifuged at 14,000 rpm for 10 minutes at 4 °C to collect the supernatant. The luciferase content in the supernatant was quantified using a luciferase assay (Promega, Madison, WI) and recorded in relative light unit per gram protein. The total protein amount was measured with the enhanced test tube protocol of the bicinchoninic acid protein assay (Pierce, Rockford, IL).

***Immunohistochemistry.*** Immunohistochemistry was performed on tissue sections to analyze incorporation of the bridge in the spinal cord after implantation, cell infiltration into the bridge, cell identification, and the distribution and identity of transfected cells. After both 1, 2, and 12 weeks,

rats ($n = 4$) were euthanized and three spinal sections each containing three to four spinal segments (T5-T7, T8-T11, and T12-L1) were retrieved, frozen in isopentane (Fisher Scientific), and stored in siliconized Eppendorf tubes at −80 °C. The tissue section containing the injury site (T8-T11) was cryopreserved in optimum cutting temperature compound and sliced longitudinally in 10-μm thick sections using a cryostat (Micron, Microm HM 505 N; Micron International, Walldorf, Germany). Every other section was collected on poly (L-lysine) coated glass slides (Fisher Scientific, Hampton, VA), postfixed, and stained.

Bridge incorporation in the spinal cord and cell infiltration into the bridge were analyzed with a hematoxylin (Surgipath Medical Industries, Richmond, IL) and eosin (Acros Organics, Morris Plains, NJ) stain, while neurofilament was stained with neurofilament 200 (NF 200; Sigma-Aldrich) as primary antibody. Spinal cords implanted with bridges containing plasmid encoding for EGFP were sectioned and stained using a double-labeling immunofluorescence staining method. All collected sections were stained with polyclonal rabbit anti-EGFP (Invitrogen, Carlsbad, CA) as a primary antibody and Alexa Fluor 488 goat anti-rabbit (green) (Invitrogen, Carlsbad, CA) as a secondary antibody. A Hoechst stain was coincidently performed with the stain for EGFP to validate the position of the cells. Every 6th collected section was double stained for a specific cell stain with primary monoclonal mouse IgG1 antibodies [(i) anti-S100 (β-subunit) for Schwann cells (Sigma); (ii) anti-oligodendrocytes (RIP) (Millipore, Billerica, MA); (iii) anti-rat monocytes/macrophages (CD68) (ED-1) (Millipore, Billerica, MA); (iv) anti-glial fibrillary acidic protein (GFAP) for reactive astrocytes (Sigma, St. Louis, MO); (v) anti-rat prolyl 4-hydroxylase (rPH) for fibroblasts (Acris Antibodies, Herford, Germany); and (vi) anti-rat RECA-1 for endothelial cells (AbD Serotec, Raleigh, NC)] and Alexa Fluor 546 goat anti-mouse (red) (Invitrogen, Carlsbad, CA) as a secondary antibody. Negative controls were performed by eliminating the primary antibodies and staining histological sections of implanted bridges without encapsulated plasmid. Pictures were taken of three random fields in the bridge and three random fields in the adjacent tissue (×20) with red and green fluorescent filter sets using Metaview software.

To determine the identity of transfected cells inside the bridge, green and red fluorescent images were overlaid in Photoshop. The percentages of transfected cells identified as a specific cell type were, based on the results, quantified for three cell types. For each cell type, 4 rats, 20 tissue sections, and 60 pictures were analyzed and counted. For each rat, every 3th collected tissue section was selected and pictures were taken in three random fields of view (×20) of the bridge. To count the number of transfected cells, an ecosse false colors 3 filter (Photoshop) was used to select the brightest 1/3 of the image, which reduced low level background staining, and a 5 by 5 grid was overlaid to mark and count the EGFP positive cells in seven random fields of the grid. Following, the green and red fluorescent images were overlaid in Photoshop and all the marked transfected cells that overlapped with the red cell stain were counted as positive for each specific cell type. Because the tissue was stained for six different cell types, every 18th collected tissue section was analyzed for each cell type. Percentages were calculated as the ratio of the transfected cells identified as a certain cell type to the total counted number of transfected cells.

***Statistics.*** Statistical analyses were performed using statistical package JMP (SAS, Cary, NC). For multiple comparisons, pairs were compared using an ANOVA with *post hoc* Tukey test with a $P$ value <0.05 defined as significant. An ANOVA with *post hoc* Wilcoxon one-way test was used to demonstrate a significant difference between experimental conditions and background levels. The error bars represent SEs in all figures.

## ACKNOWLEDGMENTS

We are grateful to Dixon Kaufman for the usage of bioluminescence imaging equipment, Rebecca Nishi for her help with the immunohistochemistry quantification, and Anna Yan and Andrew Adler for their technical assistance with the experiments. Financial support for this research was provided by the National Institutes of Health (RO1 EB005678, R21 EB006520, RO1 EB 003806) and the Christopher Reeve Paralysis Foundation (SAC2-0208-2).

## REFERENCES

1. David, S and Aguayo, AJ (1981). Axonal elongation into peripheral nervous system "bridges" after central nervous system injury in adult rats. *Science* **214**: 931–933.
2. Richardson, PM, McGuinness, UM and Aguayo, AJ (1980). Axons from CNS neurons regenerate into PNS grafts. *Nature* **284**: 264–265.
3. Geller, HM and Fawcett, JW (2002). Building a bridge: engineering spinal cord repair. *Exp Neurol* **174**: 125–136.
4. Yoshii, S, Oka, M, Shima, M, Taniguchi, A, Taki, Y and Akagi, M (2004). Restoration of function after spinal cord transection using a collagen bridge. *J Biomed Mater Res A* **70**: 569–575.
5. King, VR, Phillips, JB, Hunt-Grubbe, H, Brown, R and Priestley, JV (2005). Characterization of non-neuronal elements within fibronectin mats implanted into the damaged adult rat spinal cord. *Biomaterials* **27**: 485–496.
6. Moore, MJ, Friedman, JA, Lewellyn, EB, Mantila, SM, Krych, AJ, Ameenuddin, S *et al.* (2006). Multiple-channel scaffolds to promote spinal cord axon regeneration. *Biomaterials* **27**: 419–429.
7. Prang, P, Muller, R, Eljaouhari, A, Heckmann, K, Kunz, W, Weber, T *et al.* (2006). The promotion of oriented axonal regrowth in the injured spinal cord by alginate-based anisotropic capillary hydrogels. *Biomaterials* **27**: 3560–3569.
8. Stokols, S, Sakamoto, J, Breckon, C, Holt, T, Weiss, J and Tuszynski, MH (2006). Templated agarose scaffolds support linear axonal regeneration. *Tissue Eng* **12**: 2777–2787.
9. Stokols, S and Tuszynski, MH (2006). Freeze-dried agarose scaffolds with uniaxial channels stimulate and guide linear axonal growth following spinal cord injury. *Biomaterials* **27**: 443–451.
10. Yang, Y, De Laporte, L, Rives, CB, Jang, JH, Lin, WC, Shull, KR *et al.* (2005). Neurotrophin releasing single and multiple lumen nerve conduits. *J Control Release* **104**: 433–446.
11. Willerth, SM and Sakiyama-Elbert, SE (2007). Approaches to neural tissue engineering using scaffolds for drug delivery. *Adv Drug Deliv Rev* **59**: 325–338.
12. Houweling, DA, Lankhorst, AJ, Gispen, WH, Bar, PR and Joosten, EA (1998). Collagen containing neurotrophin-3 (NT-3) attracts regrowing injured corticospinal axons in the adult rat spinal cord and promotes partial functional recovery. *Exp Neurol* **153**: 49–59.
13. Taylor, SJ, Rosenzweig, ES, McDonald, JW 3rd and Sakiyama-Elbert, SE (2006). Delivery of neurotrophin-3 from fibrin enhances neuronal fiber sprouting after spinal cord injury. *J Control Release* **113**: 226–235.
14. Houle, JD, Tom, VJ, Mayes, D, Wagoner, G, Phillips, N and Silver, J (2006). Combining an autologous peripheral nervous system "bridge" and matrix modification by chondroitinase allows robust, functional regeneration beyond a hemisection lesion of the adult rat spinal cord. *J Neurosci* **26**: 7405–7415.
15. De Laporte, L and Shea, LD (2007). Matrices and scaffolds for DNA delivery in tissue engineering. *Adv Drug Deliv Rev* **59**: 292–307.
16. Jang, JH, Rives, CB and Shea, LD (2005). Plasmid delivery *in vivo* from porous tissue-engineering scaffolds: transgene expression and cellular transfection. *Mol Ther* **12**: 475–483.
17. Huang, YC, Riddle, K, Rice, KG and Mooney, DJ (2005). Long-term *in vivo* gene expression via delivery of PEI-DNA condensates from porous polymer scaffolds. *Hum Gene Ther* **16**: 609–617.
18. Berry, M, Gonzalez, AM, Clarke, W, Greenlees, L, Barrett, L, Tsang, W *et al.* (2001). Sustained effects of gene-activated matrices after CNS injury. *Mol Cell Neurosci* **17**: 706–716.
19. Shea, LD, Smiley, E, Bonadio, J and Mooney, DJ (1999). DNA delivery from polymer matrices for tissue engineering. *Nat Biotechnol* **17**: 551–554.
20. Teng, YD, Lavik, EB, Qu, X, Park, KI, Ourednik, J, Zurakowski, D *et al.* (2002). Functional recovery following traumatic spinal cord injury mediated by a unique polymer scaffold seeded with neural stem cells. *Proc Natl Acad Sci USA* **99**: 3024–3029.
21. Friedman, JA, Windebank, AJ, Moore, MJ, Spinner, RJ, Currier, BL and Yaszemski, MJ (2002). Biodegradable polymer grafts for surgical repair of the injured spinal cord. *Neurosurgery* **51**: 742–751; discussion 751–742.
22. Gautier, SE, Oudega, M, Fragoso, M, Chapon, P, Plant, GW, Bunge, MB *et al.* (1998). Poly(alpha-hydroxyacids) for application in the spinal cord: resorbability and biocompatibility with adult rat Schwann cells and spinal cord. *J Biomed Mater Res* **42**: 642–654.
23. Schnell, L, Schneider, R, Kolbeck, R, Barde, YA and Schwab, ME (1994). Neurotrophin-3 enhances sprouting of corticospinal tract during development and after adult spinal cord lesion. *Nature* **367**: 170–173.
24. Bradbury, EJ, Khemani, S, Von, R, King, Priestley, JV and McMahon, SB (1999). NT-3 promotes growth of lesioned adult rat sensory axons ascending in the dorsal columns of the spinal cord. *Eur J Neurosci* **11**: 3873–3883.
25. Koda, M, Hashimoto, M, Murakami, M, Yoshinaga, K, Ikeda, O, Yamazaki, M *et al.* (2004). Adenovirus vector-mediated *in vivo* gene transfer of brain-derived neurotrophic factor (BDNF) promotes rubrospinal axonal regeneration and functional recovery after complete transection of the adult rat spinal cord. *J Neurotrauma* **21**: 329–337.
26. Jimenez Hamann, MC, Tator, CH and Shoichet, MS (2005). Injectable intrathecal delivery system for localized administration of EGF and FGF-2 to the injured rat spinal cord. *Exp Neurol* **194**: 106–119.
27. Wong, DY, Leveque, JC, Brumblay, H, Krebsbach, PH, Hollister, SJ and Lamarca, F (2008). Macro-architectures in spinal cord scaffold implants influence regeneration. *J Neurotrauma* **25**: 1027–1037.

28. Chen, MS, Huber, AB, van der Haar, ME, Frank, M, Schnell, L, Spillmann, AA *et al.* (2000). Nogo-A is a myelin-associated neurite outgrowth inhibitor and an antigen for monoclonal antibody IN-1. *Nature* **403**: 434–439.
29. Talbott, JF, Cao, Q, Bertram, J, Nkansah, M, Benton, RL, Lavik, E *et al.* (2007). CNTF promotes the survival and differentiation of adult spinal cord-derived oligodendrocyte precursor cells *in vitro* but fails to promote remyelination *in vivo*. *Exp Neurol* **204**: 485–489.
30. Einstein, O, Ben-Menachem-Tzidon, O, Mizrachi-Kol, R, Reinhartz, E, Grigoriadis, N and Ben-Hur, T (2006). Survival of neural precursor cells in growth factor-poor environment: implications for transplantation in chronic disease. *Glia* **53**: 449–455.
31. Zhang, X, Zeng, Y, Zhang, W, Wang, J, Wu, J and Li, J (2007). Co-transplantation of neural stem cells and NT-3-overexpressing Schwann cells in transected spinal cord. *J Neurotrauma* **24**: 1863–1877.
32. Xu, XM, Guenard, V, Kleitman, N, Aebischer, P and Bunge, MB (1995). A combination of BDNF and NT-3 promotes supraspinal axonal regeneration into Schwann cell grafts in adult rat thoracic spinal cord. *Exp Neurol* **134**: 261–272.
33. Langer, R (1998). Drug delivery and targeting. *Nature* **392**: 5–10.
34. Blits, B, Dijkhuizen, PA, Boer, GJ and Verhaagen, J (2000). Intercostal nerve implants transduced with an adenoviral vector encoding neurotrophin-3 promote regrowth of injured rat corticospinal tract fibers and improve hindlimb function. *Exp Neurol* **164**: 25–37.
35. Geisert, EE Jr, Del Mar, NA, Owens, JL and Holmberg, EG (1995). Transfecting neurons and glia in the rat using pH-sensitive immunoliposomes. *Neurosci Lett* **184**: 40–43.
36. Takahashi, K, Schwarz, E, Ljubetic, C, Murray, M, Tessler, A and Saavedra, RA (1999). DNA plasmid that codes for human Bcl-2 gene preserves axotomized Clarke's nucleus neurons and reduces atrophy after spinal cord hemisection in adult rats. *J Comp Neurol* **404**: 159–171.
37. Shimamura, M, Sato, N, Taniyama, Y, Kurinami, H, Tanaka, H, Takami, T *et al.* (2005). Gene transfer into adult rat spinal cord using naked plasmid DNA and ultrasound microbubbles. *J Gene Med* **7**: 1468–1474.
38. Mannes, AJ, Caudle, RM, O'Connell, BC and Iadarola, MJ (1998). Adenoviral gene transfer to spinal-cord neurons: intrathecal vs. intraparenchymal administration. *Brain Res* **793**: 1–6.
39. Grill, R, Murai, K, Blesch, A, Gage, FH and Tuszynski, MH (1997). Cellular delivery of neurotrophin-3 promotes corticospinal axonal growth and partial functional recovery after spinal cord injury. *J Neurosci* **17**: 5560–5572.
40. Nakahara, Y, Gage, FH and Tuszynski, MH (1996). Grafts of fibroblasts genetically modified to secrete NGF, BDNF, NT-3, or basic FGF elicit differential responses in the adult spinal cord. *Cell Transplant* **5**: 191–204.
41. Tuszynski, MH, Grill, R, Jones, LL, Brant, A, Blesch, A, Low, K *et al.* (2003). NT-3 gene delivery elicits growth of chronically injured corticospinal axons and modestly improves functional deficits after chronic scar resection. *Exp Neurol* **181**: 47–56.
42. Wake, MC, Patrick, CW Jr and Mikos, AG (1994). Pore morphology effects on the fibrovascular tissue growth in porous polymer substrates. *Cell Transplant* **3**: 339–343.
43. Blight, AR (1992). Macrophages and inflammatory damage in spinal cord injury. *J Neurotrauma* **9** (suppl. 1): S83–S91.
44. Hyde, SC, Pringle, IA, Abdullah, S, Lawton, AE, Davies, LA, Varathalingam, A *et al.* (2008). CpG-free plasmids confer reduced inflammation and sustained pulmonary gene expression. *Nat Biotechnol* **26**: 549–551.
45. Jang, JH and Shea, LD (2006). Intramuscular delivery of DNA releasing microspheres: microsphere properties and transgene expression. *J Control Release* **112**: 120–128.
46. Kapur, TA and Shoichet, MS (2004). Immobilized concentration gradients of nerve growth factor guide neurite outgrowth. *J Biomed Mater Res A* **68**: 235–243.
47. Houchin-Ray, T, Whittlesey, KJ and Shea, LD (2007). Spatially patterned gene delivery for localized neuron survival and neurite extension. *Mol Ther* **15**: 705–712.
48. Bracken, MB (2001). Methylprednisolone and acute spinal cord injury: an update of the randomized evidence. *Spine* **26**: S47–S54.
49. Cummings, BJ, Uchida, N, Tamaki, SJ, Salazar, DL, Hooshmand, M, Summers, R *et al.* (2005). Human neural stem cells differentiate and promote locomotor recovery in spinal cord-injured mice. *Proc Natl Acad Sci USA* **102**: 14069–14074.
50. Harris, LD, Kim, BS and Mooney, DJ (1998). Open pore biodegradable matrices formed with gas foaming. *J Biomed Mater Res* **42**: 396–402.